Hydrodynamics and two-dimensional dark lump solitons for polariton superfluids

D. J. Frantzeskakis,[1] T. P. Horikis,[2] A. S. Rodrigues,[3] P. G. Kevrekidis,[4] R. Carretero-González,[5] and J. Cuevas-Maraver[6]

[1]*Department of Physics, National and Kapodistrian University of Athens, Panepistimiopolis, Zografos, Athens 15784, Greece*

[2]*Department of Mathematics, University of Ioannina, Ioannina 45110, Greece*

[3]*Departamento de Física e Astronomia/CFP, Faculdade de Ciências, Universidade do Porto, R. Campo Alegre, 687-4169-007 Porto, Portugal*

[4]*Department of Mathematics and Statistics, University of Massachusetts, Amherst, Massachusetts 01003-4515, USA*

[5]*Nonlinear Dynamical Systems Group, Computational Sciences Research Center, and Department of Mathematics and Statistics, San Diego State University, San Diego, California 92182-7720, USA*

[6]*Grupo de Física No Lineal, Departamento de Física Aplicada I, Universidad de Sevilla. Escuela Politécnica Superior, C/ Virgen de África, 7, 41011-Sevilla, Spain and Instituto de Matemáticas de la Universidad de Sevilla (IMUS). Edificio Celestino Mutis. Avda. Reina Mercedes s/n, 41012-Sevilla, Spain*

(Received 23 April 2018; published 8 August 2018)

We study a two-dimensional incoherently pumped exciton-polariton condensate described by an open-dissipative Gross-Pitaevskii equation for the polariton dynamics coupled to a rate equation for the exciton density. Adopting a hydrodynamic approach, we use multiscale expansion methods to derive several models appearing in the context of shallow water waves with viscosity. In particular, we derive a Boussinesq/Benney-Luke–type equation and its far-field expansion in terms of Kadomtsev-Petviashvili-I (KP-I) equations for right- and left-going waves. From the KP-I model, we predict the existence of vorticity-free, weakly (algebraically) localized two-dimensional dark-lump solitons. We find that, in the presence of dissipation, dark lumps exhibit a lifetime three times larger than that of planar dark solitons. Direct numerical simulations show that dark lumps do exist, and their dissipative dynamics is well captured by our analytical approximation. It is also shown that lumplike and vortexlike structures can spontaneously be formed as a result of the transverse "snaking" instability of dark soliton stripes.

DOI: 10.1103/PhysRevE.98.022205

I. INTRODUCTION

Exciton-polariton superfluids, composed by hybrid light-matter quasi-particles emerging in the regime of strong coupling, offer unique opportunities for studies on quantum, nonequilibrium and nonlinear dynamics [1,2]. Being intrinsically lossy—and hence being continuously replenished in order to be sustained—polariton superfluids are described by damped-driven versions of the Gross-Pitaevskii (GP) equation [3–7] (see also the review of Ref. [2]). Such models have been successfully used for the theoretical study of fundamental nonlinear phenomena that have been observed in experiments, e.g., the formation and dynamics of quantized vortices [8–11] and dark solitons [12–18].

There are numerous works that have studied the dynamics of dark solitons in polariton condensates. For instance, dark solitons in polariton condensates coherently and resonantly driven by a pumping laser were studied in Refs. [19–21]. Also, in the presence of nonresonant pumping, simplified Ginzburg-Landau models [6,7] were used to describe one-dimensional (1D) dark solitons and two-dimensional (2D) ring dark solitons in Refs. [22,23]. In the same case (of nonresonant pumping), and using the open-dissipative GP model of Refs. [3–5], which involves the coupling of polaritons to the exciton reservoir, dark polariton solitons were analyzed using an adiabatic approximation [24] and variational techniques [25,26]. Finally, in Ref. [27], the 1D open-dissipative GP model was asymptotically reduced to an effective Korteweg-de Vries (KdV) equation with linear loss, which was then used to describe dark soliton dynamics in polariton superfluids.

The recent work of Ref. [27] suggests a number of interesting questions. Before asking some of these, it is relevant to mention the following. The KdV equation is known to be a universal model describing shallow water waves [28], as well as ion-acoustic solitons in plasmas [29], solitons in mechanical and electrical lattices, and so on [30]. The KdV equation describes uni-directional propagation and stems, as the far-field limit, from bi-directional models appearing in various contexts—predominantly in shallow water waves—such as the Boussinesq [28–30] and the Benney-Luke (BL) [31] equations. Additionally, the generalization of the KdV in the 2D setting, namely the Kadomtsev-Petviashvili (KP) equation, also stems from the 2D versions of Boussinesq- and BL-type models [28]. Then, one can ask whether these models may be relevant to the context of polariton superfluids as well. If yes, one can hope to use them towards predicting dynamical features of the solitons, towards identifying novel—e.g., 2D—solitonic structures in exciton-polariton systems and, finally, towards quantifying the role of the open-dissipative nature of these systems.

The scope of this work is to address these questions. In particular, our starting point is the open-dissipative GP equation of Refs. [3–5] in 2D, which is perhaps the most customary approach for describing an incoherently pumped exciton-polariton BEC. This model is composed by a dissipative GP equation for the macroscopic wavefunction of the polariton condensate, coupled with a rate equation for the exciton reservoir density. Adopting a hydrodynamic description, we use multiscale expansion methods to derive—under certain physically relevant

conditions—asymptotic reductions of the open-dissipative GP equation. Specifically, at an intermediate stage of the asymptotic analysis, we obtain a Boussinesq/BL-type equation with linear loss—similarly to the case of shallow water waves when viscosity is taken into account [32,33]. Next, we consider the far-field of the Boussinesq/BL-type equation, and derive a pair of Kadomtsev-Petviashvili (KP) equations [34] with linear loss, for right- and left-going waves. Such KP models (and also their 1D, KdV, counterpart) perturbed by a linear loss term have been used in shallow water wave settings involving straits of nonuniform water depth [35,36]. Importantly, given the self-defocusing nature of the nonlinearity, the derived KP model is of the KP-I type, i.e., it is characterized by positive dispersion, and arises in the context of shallow water waves, or in liquid thin films, when surface tension dominates gravity [28].

Next, in the absence of dissipation, 1D line soliton and 2D lump solutions of the KP-I equation [37] are used for the construction of two different types of (approximate) soliton solutions of the original open-dissipative GP model: (i) planar dark solitons, satisfying the 1D (KdV) counterpart of the KP-I—similar to the ones studied in the 1D setting of Ref. [27]—and (ii) weakly localized (i.e., algebraically decaying), vorticity-free, 2D dark solitons. The fact that the underlying KP equation is of the KP-I type has important consequences: since line solitons (lumps) of the KP-I are unstable (stable) [38] then, in the original GP model, planar dark solitons are also unstable in 2D—as was also demonstrated in the simulations of Ref. [24]—while 2D dark lump solitons are dynamically robust. Importantly, similar dark lump solitons have been predicted and studied in nonlinear optics [39–41], atomic Bose-Einstein condensates (BECs) [42] (see also the reviews [43]), superfluid Fermi gases [44], and in laser-plasma interactions [45]. As was shown, these structures can emerge as a result of the slowly developing transverse (alias "snaking") instability of the 1D dark solitons [46], or during vortex-antivortex annihilation [47] (see also relevant work in Refs. [48–50]).

We also study the role of dissipation on the soliton dynamics, which is particularly relevant due to the open-dissipative nature of the present system. It is found that the amplitude of both the line solitons and the lumps decays exponentially in time, with a rate which is set by physical parameters of the problem, namely the polariton decay rate and the relative deviation of the uniform pumping from its threshold value. Remarkably, it is found that the lifetime of the weakly localized dark lump soliton is three times larger than the one of the line soliton. This suggests that these structures have a good chance to be observed in experiments. Finally, we use direct numerical simulations to show that dark lumps do exist, and their dissipative dynamics is well described by our asymptotic approach. In addition, the use of direct simulations shows that relevant lump—as well as vortical—structures can spontaneously be formed as a result of the transverse "snaking" instability of weak dark soliton stripes.

The paper is structured as follows. In Sec. II, we present the model and use asymptotic expansion methods to derive the effective Boussinesq/BL and KP-I equations. In Sec. III, employing the soliton solutions of the KP-I model, we construct corresponding approximate soliton solutions of the open-dissipative GP equation. We also present results of direct numerical simulations depicting: (i) the dissipative dynamics of the dark lumps, as well as (ii) the snaking instability of dark soliton stripes. Finally, Sec. IV summarizes our conclusions and provides directions for relevant future work.

II. THE MODEL AND ITS ANALYTICAL CONSIDERATION

A. The open-dissipative Gross-Pitaevskii model

Let us consider a 2D incoherently pumped (far from resonance) exciton-polariton condensate described, in the mean-field approximation, by a generalized open-dissipative GP system where the polariton wave function $\Psi(\boldsymbol{r},t)$ is coupled to a rate equation for the exciton reservoir density $n(\boldsymbol{r},t)$ [3–5]:

$$i\hbar\Psi_t = \left[-\frac{\hbar^2}{2M}\Delta + g_C|\Psi|^2 + g_R n + \frac{i\hbar}{2}(Rn-\gamma_C)\right]\Psi, \tag{1}$$

$$n_t = P(\boldsymbol{r},t) - (\gamma_R + R|\Psi|^2)n, \tag{2}$$

where subscripts in the fields Ψ and n denote partial derivatives and $\Delta \equiv \partial_x^2 + \partial_y^2$ is the 2D Laplacian. In these equations, the polaritons, with effective mass (lower polariton branch) M, have a (self) nonlinear interaction strength g_C and are coupled, with coupling strength g_R, to the exciton reservoir. Furthermore, R measures the reservoir's rate of stimulated scattering, while γ_C and γ_R are the polariton and exciton loss rates, respectively. Finally, $P(\boldsymbol{r},t)$ is the exciton creation rate induced by the spatio-temporal laser pumping profile. Note that within this model, the polariton condensate includes an intrinsic repulsive (defocusing) nonlinearity ($g_C > 0$). It is worthwhile to point out that while we restrict considerations to the repulsive nonlinearity herein, a more detailed view of the dispersion relation of the (lower) polariton branch is of interest in its own right. This is true not only due to the potentially different character of the waves produced, but also due to the possibility of generating optical parametric instabilities in the system [51].

The open-dissipative GP system Eqs. (1) and (2) belongs to a class of models where an equation describing a pumped reservoir is coupled to a GP-like equation. Such models are usually referred to as "diffusive models" [52], due to the diffusive nature of their dispersion relation; this, however, is not compatible with the superfluidity of exciton-polaritons observed in experiments (see, e.g., Refs. [53]). The present model is expected to be valid in the vicinity of the spectral band edge and to be able to capture associated nonlinear phenomena. Nevertheless, alternative models that cope with the superfluidity in non-resonantly pumped systems have also been presented [52].

To proceed further, first we express Eqs. (1) and (2) in dimensionless form by: scaling space in terms of the healing length $\bar{\xi} = \hbar/\sqrt{Mg_C n_C}$ (where n_C is the background's condensate density), time in units of $t_0 = \bar{\xi}/c_S$ (where $c_S = \sqrt{g_C n_C/M}$ is the speed of sound), and densities (namely $|\Psi|^2$ and n) in terms of n_C. Using these scalings yields:

$$i\Psi_t = -\frac{1}{2}\Delta\Psi + |\Psi|^2\Psi + g_R n\Psi + \frac{i}{2}(Rn-\gamma_C)\Psi, \tag{3}$$

$$n_t = P(\boldsymbol{r},t) - (\gamma_R + R|\Psi|^2)n, \tag{4}$$

where now g_R and R are measured in units of g_C and $g_C/\hbar$, respectively, γ_C and γ_R are measured in units of $1/t_0$, and the laser pump $P(x,t)$ is measured in units of n_C/t_0.

The starting step to describe the polariton condensate as a fluid is to employ the so-called Madelung transformation $\Psi = \sqrt{\rho}\exp(i\varphi)$ that expresses the polariton evolution in terms of its density ρ and phase φ. Then, after separating real and imaginary parts, one obtains the fluidlike equations:

$$\varphi_t + \rho + \tfrac{1}{2}(\nabla\varphi)^2 - \tfrac{1}{2}\rho^{-1/2}\Delta\rho^{1/2} + g_R n = 0, \quad (5)$$

$$\rho_t + \nabla\cdot(\rho\nabla\varphi) - (Rn - \gamma_C)\rho = 0, \quad (6)$$

$$n_t - P + (\gamma_R + R\rho)n = 0, \quad (7)$$

where $\nabla \equiv (\partial_x, \partial_y)$ is the gradient operator. From this point onward, we restrict our attention to the constant-in-time and spatially uniform pumping profile $P(x,t) = P_0$. For this pumping profile the spatially homogeneous steady states of the exciton-polariton system correspond to

$$\rho = \rho_0, \quad n = n_0, \quad \varphi = -\mu t, \quad (8)$$

where the steady-state condensate and reservoir background densities, ρ_0 and n_0, as well as the chemical potential μ, are given by [3,24,27]

$$\rho_0 = \frac{P_0 - P_0^{(\mathrm{th})}}{\gamma_C}, \quad n_0 = \frac{\gamma_C}{R}, \quad \mu = \rho_0 + \frac{g_R\gamma_C}{R}, \quad (9)$$

where we have defined

$$P_0^{(\mathrm{th})} \equiv \frac{\gamma_R\gamma_C}{R}. \quad (10)$$

In the above, the inequality $P_0 > P_0^{(\mathrm{th})}$ must be satisfied for the polariton density to be meaningful (i.e., positive). This implies that a nonzero polariton steady-state can only be sustained provided that the pump strength P_0 exceeds the threshold value $P_0^{(\mathrm{th})}$ given above. Therefore, by defining the following positive parameter, corresponding to the relative deviation of the pumping from the threshold,

$$\alpha = \frac{P_0 - P_0^{(\mathrm{th})}}{P_0^{(\mathrm{th})}}, \quad (11)$$

we can express the equilibrium condensate density as $\rho_0 = (\gamma_R/R)\alpha$.

Let us consider the case $\gamma_C \ll \gamma_R$ corresponding to the physically relevant scenario whereby the exciton reservoir follows adiabatically the polariton condensate evolution [3]. Here, however, it is important to mention that physical systems may not always fall in this regime: for instance, a reservoir-mediated dynamical instability of a nonequilibrium exciton-polariton condensate that was recently demonstrated experimentally [54], can occur only in the nonadiabatic regime. Nevertheless, for our investigations, we will focus on the adiabatic regime and employ a multiscale expansion approach, following the smallness of the relevant quantities. This will be done by introducing the formal small parameter $0 < \epsilon \ll 1$ and assume that $\gamma_C = \epsilon\tilde{\gamma}_C$, where $\tilde{\gamma}_C$ and γ_R remain of order $\mathcal{O}(1)$. By the same token, we consider that the reservoir's scattering rate R and the relative deviation of the pumping from the threshold, α, are also relatively small [24] and of order ϵ: $R = \epsilon\tilde{R}$ and $\alpha = \epsilon\tilde{\alpha}$, where $\tilde{R}$ and $\tilde{\alpha}$ are of order $\mathcal{O}(1)$. All other parameters and relevant quantities—such as the densities ρ_0 and n_0, the pump threshold $P_0^{(\mathrm{th})}$, and the chemical potential μ—are of order $\mathcal{O}(1)$.

B. Effective nonlinear evolution equations

1. The Boussinesq/Benney-Luke–type equation

To better underline the hydrodynamic origin of the soliton solutions presented below, we will first derive a Boussinesq/Benney-Luke–type equation. We thus seek solutions of Eqs. (5)–(7) in the form of the following asymptotic expansions:

$$\varphi = -\mu t + \epsilon^{1/2}\Phi, \quad (12a)$$

$$\rho = \rho_0 + \epsilon\rho_1 + \epsilon^2\rho_2 + \cdots, \quad (12b)$$

$$n = n_0 + \epsilon^2 n_1 + \epsilon^3 n_2 + \cdots, \quad (12c)$$

where ϵ is the same formal small parameter used for the scaling of the parametric dependences above, while the unknown real functions Φ, ρ_j and n_j $(j = 1, 2, \ldots)$ are assumed to depend on the slow variables:

$$X = \epsilon^{1/2}x, \quad Y = \epsilon^{1/2}y, \quad T = \epsilon^{1/2}t. \quad (13)$$

Substituting the expansion Eqs. (12a)–(12c) into Eqs. (5)–(7), and using the variables in Eq. (13), we obtain the following results. First, up to order $\mathcal{O}(\epsilon)$, Eq. (5) reads

$$\Phi_T + \rho_1 + \epsilon\left[\frac{1}{2}(\tilde{\nabla}\Phi)^2 - \frac{1}{4\rho_0}\tilde{\Delta}\rho_1 + \rho_2\right] = 0, \quad (14)$$

where $\tilde{\Delta} = \partial_X^2 + \partial_Y^2$ and $\tilde{\nabla} = (\partial_X, \partial_Y)$. Second, Eq. (6) leads, at orders $\mathcal{O}(\epsilon^{3/2})$ and $\mathcal{O}(\epsilon^{5/2})$, to the following equations, respectively:

$$\rho_{1T} + \rho_0\tilde{\Delta}\Phi = 0, \quad (15)$$

$$\rho_{2T} + \tilde{\nabla}\cdot(\rho_1\tilde{\nabla}\Phi) = 0. \quad (16)$$

Third, Eq. (7), at the leading order in ϵ, i.e., at order $\mathcal{O}(\epsilon^2)$, yields:

$$n_1 = -\frac{\tilde{\gamma}_C}{\gamma_R}\rho_1, \quad (17)$$

connecting the reservoir density n_1 to the polariton density ρ_1. Obviously, once ρ_1 is found, then n_1 and Φ can be, respectively, derived from Eq. (17) and the leading-order part of Eq. (14), namely $\Phi_T + \rho_1 = 0$.

At the present order of approximation, Eqs. (14)–(16) do not incorporate dissipative terms. The lowest-order such term appears in Eq. (16), and has the form $-\epsilon^3\tilde{\alpha}\gamma_R n_1$, i.e., it is a term of order $\mathcal{O}(\epsilon^3)$. To take into account this term, we may modify Eq. (16) by adding to its right-hand side the additional term $-\epsilon^{1/2}\tilde{\alpha}\gamma_R n_1$. Taking into regard this modification, we may proceed as follows. Using Eq. (15) and the modified Eq. (16), we can eliminate the functions $\rho_{1,2}$ from Eq. (14) and derive the following equation for Φ:

$$\Phi_{TT} - C^2\tilde{\Delta}\Phi + \epsilon\left[\tfrac{1}{4}\tilde{\Delta}^2\Phi + \tfrac{1}{2}\partial_T(\tilde{\nabla}\Phi)^2 + \tilde{\nabla}\cdot(\Phi_T\tilde{\nabla}\Phi)\right] + \epsilon^{3/2}\tilde{\alpha}\tilde{\gamma}_C\Phi_T = 0, \quad (18)$$

where the squared velocity C^2 is given by

$$C^2 = \rho_0, \tag{19}$$

up to corrections of $\mathcal{O}(\epsilon^2)$.

It is clear that, to leading-order, Eq. (18) is a linear wave equation. In addition, at $\mathcal{O}(\epsilon)$, Eq. (18) incorporates fourth-order dispersion terms and quadratic nonlinear terms. Obviously, Eq. (18) resembles the Boussinesq and Benney-Luke [31] equations, which describe bidirectional shallow water waves, in the framework of small-amplitude and long-wavelength approximations [28]; note that such Boussinesq-type models have also been used in other contexts, ranging from ion-acoustic waves in plasmas [29] to mechanical lattices and electrical transmission lines [30]. Finally, at the order $\mathcal{O}(\epsilon^{3/2})$, Eq. (18) also includes a dissipative term (see below) proportional to $\tilde{\alpha}\tilde{\gamma}_C$, i.e., depending on the polariton decay rate and the relative deviation of the uniform pumping from its threshold value. Such a Boussinesq-like model with constant dissipation can also be derived in the context of shallow water waves, upon incorporating a dissipative term—to account for the presence of viscosity—in the free-surface dynamical boundary condition [32] (see also Ref. [33]).

Before proceeding further, it is relevant to focus, at first, on the linear dispersion relation of Eq. (18). Seeking small-amplitude solutions of Eq. (18) behaving like $\Phi \propto \exp[i(\boldsymbol{k}\cdot\boldsymbol{r}-\omega t)]$, with $\boldsymbol{r}=(x,y)$, we find that the perturbations' wave vector $\boldsymbol{k}=(k_x,k_y)$ and frequency ω obey the dispersion relation:

$$\omega(|\boldsymbol{k}|) = \pm\sqrt{\omega_B^2(|\boldsymbol{k}|) - \left(\frac{1}{2}\epsilon^{3/2}\tilde{\alpha}\tilde{\gamma}_C\right)^2} - \frac{i}{2}\epsilon^{3/2}\tilde{\alpha}\tilde{\gamma}_C, \tag{20}$$

where $\omega_B^2(|\boldsymbol{k}|) = |\boldsymbol{k}|^2C^2 + (1/4)\epsilon|\boldsymbol{k}|^4$ is the standard Bogoliubov dispersion relation for a condensate at equilibrium [43]. It is clear that Eq. (20) suggests a decay rate of linear waves proportional to $\tilde{\alpha}\tilde{\gamma}_C$. Below we will show that localized nonlinear waves, in the form of 1D line solitons and 2D lumps, satisfying a KP-I equation that will be derived as the far field of Eq. (18), also feature a decay rate proportional to $\tilde{\alpha}\tilde{\gamma}_C$. This can also be suggested by the linear theory as follows. Using $|\boldsymbol{k}|^2 = k_x^2 + k_y^2$, and keeping terms up to the order $\mathcal{O}(\epsilon^2)$, we cast Eq. (20) into the form:

$$\omega \approx \pm Ck_x\left(1+\frac{k_y^2}{k_x^2}\right)^{1/2}\left[1+\frac{\epsilon}{4C^2}k_x^2\left(1+\frac{k_y^2}{k_x^2}\right)\right]^{1/2} - \frac{i}{2}\epsilon^{3/2}\tilde{\alpha}\tilde{\gamma}_C, \tag{21}$$

with $\pm$ corresponding to right- and left-going waves. Then, considering a quasi-2D evolution with $k_y/k_x = \mathcal{O}(\epsilon^{1/2})$, we may further simplify Eq. (21) to yield:

$$\frac{1}{C}\omega k_x = \pm\left(k_x^2 + \frac{\epsilon}{8C^2}k_x^4 + \frac{\epsilon}{2}k_y^2\right) - \frac{i}{2C}\epsilon^{3/2}\tilde{\alpha}\tilde{\gamma}_C k_x. \tag{22}$$

Then, using $\omega \to i\partial_t$, $k_{x,y} \to -i\partial_{x,y}$, it is found that the linear PDE associated with this dispersion relation is: $\partial_x[\pm q_t + Cq_x - (\epsilon/8C)q_{xxx}] + (\epsilon C/2)q_{yy} = \mp\epsilon^{3/2}\tilde{\alpha}\tilde{\gamma}_C q_x$. To this end, employing the transformation $x' = x - Ct$ and using the slow time $t' = \epsilon t$, the above equation takes the form

$$\partial_{x'}\left(\pm q_{t'} - \frac{1}{8C}q_{x'x'x'}\right) + \frac{C}{2}q_{yy} = \mp\frac{1}{2}\epsilon^{1/2}\tilde{\alpha}\tilde{\gamma}_C q_{x'}, \tag{23}$$

which is a linear KP equation incorporating, in its right-hand side, a small [of order $\mathcal{O}(\epsilon^{1/2})$] linear loss term. To derive the full nonlinear version of the KP model, in the next section, we resort to the method of multiple scales.

2. *The Kadomtsev-Petviashvili-I equation*

We now proceed to derive the far-field equations stemming from Eq. (18), in the framework of multiscale asymptotic expansions. As is well known, the far-field of the Boussinesq equation in $(1+1)$-dimensions is a pair of KdV equations [28], while in $(2+1)$-dimensions, it is a pair of KP equations [55–57], for right- and left-going waves. The KP equation, can be derived under the additional assumptions of quasi-two-dimensionality and unidirectional propagation. In particular, first we introduce the asymptotic expansion:

$$\Phi = \Phi_0 + \epsilon\Phi_1 + \cdots, \tag{24}$$

where the unknown functions Φ_ℓ ($\ell = 0, 1, \ldots$) depend on the variables

$$\xi = X - CT,\ \eta = X + CT,\quad \mathcal{Y} = \epsilon^{1/2}Y,\quad \mathcal{T} = \epsilon T.$$

Substituting this expansion into Eq. (18), at the leading-order in ϵ, we obtain the wave equation

$$\Phi_{0\xi\eta} = 0, \tag{25}$$

implying that Φ_0 can be expressed as a superposition of a right-going wave, $\Phi_0^{(R)}$, depending on ξ, and a left-going one, $\Phi_0^{(L)}$, depending on η, namely:

$$\Phi_0 = \Phi_0^{(R)}(\xi,\mathcal{Y},\mathcal{T}) + \Phi_0^{(L)}(\eta,\mathcal{Y},\mathcal{T}). \tag{26}$$

In addition, at order $\mathcal{O}(\epsilon)$, and taking into regard—as before—the correction including the dissipative term of order $\mathcal{O}(\epsilon^{3/2})$ [cf. last term in the left-hand side of Eq. (18)], we obtain the equation

$$\begin{aligned}4C^2\Phi_{1\xi\eta} = &-C\left(\Phi_{0\xi\xi}^{(R)}\Phi_{0\eta}^{(L)} - \Phi_{0\xi}^{(R)}\Phi_{0\eta\eta}^{(L)}\right) + \left[\partial_\xi\left(-2C\Phi_{0\mathcal{T}}^{(R)} + \frac{1}{4}\Phi_{0\xi\xi\xi}^{(R)} - \frac{3C}{2}\Phi_{0\xi}^{(R)2} - \epsilon^{1/2}C\tilde{\alpha}\tilde{\gamma}_C\Phi_0^{(R)}\right) - C^2\Phi_{0\mathcal{Y}\mathcal{Y}}^{(R)}\right]\\ &+\left[\partial_\eta\left(2C\Phi_{0\mathcal{T}}^{(L)} + \frac{1}{4}\Phi_{0\tilde{\eta}\tilde{\eta}\tilde{\eta}}^{(L)} + \frac{3C}{2}\Phi_{0\tilde{\eta}}^{(L)2} + \epsilon^{1/2}C\tilde{\alpha}\tilde{\gamma}_C\Phi_0^{(L)}\right) - C^2\Phi_{0\mathcal{Y}\mathcal{Y}}^{(L)}\right].\end{aligned} \tag{27}$$

When integrating Eq. (27), secular terms arise from the square brackets in the right-hand side, which are functions of ξ or η alone, not both. Removal of these secular terms leads to two uncoupled nonlinear evolution equations for $\Phi_0^{(R)}$ and $\Phi_0^{(L)}$. Furthermore, using the equation $\Phi_T = -\rho_1$, obtained from the leading-order part of Eq. (14), the amplitude ρ_1

is also decomposed to a left- and a right-going wave, i.e., $\rho_1 = \rho_1^{(R)} + \rho_1^{(L)}$, with

$$C\Phi_{0\xi}^{(R)} = \rho_1^{(R)}, \quad C\Phi_{0\eta}^{(L)} = -\rho_1^{(L)}. \tag{28}$$

To this end, using the above equations for $\Phi_0^{(R)}$ and $\Phi_0^{(L)}$, along with Eqs. (28), yields the following KP equations for $\rho_1^{(R,L)}$:

$$\partial_{\mathcal{X}}\left(\pm\rho_{1\mathcal{T}}^{(R,L)} - \frac{\alpha}{8C}\rho_{1\mathcal{X}\mathcal{X}\mathcal{X}}^{(R,L)} + \frac{3C}{2}\rho_1^{(R,L)}\rho_{1\mathcal{X}}^{(R,L)}\right) + \frac{1}{2}C\rho_{1\mathcal{Y}\mathcal{Y}}^{(R,L)} = \mp\frac{1}{2}\epsilon^{1/2}\tilde{\alpha}\tilde{\gamma}_C\rho_{1\mathcal{X}}^{(R,L)}, \tag{29}$$

where $\mathcal{X} = \xi$ or $\mathcal{X} = \eta$, as well as $\pm$, corresponds to the right (R)- or the left (L)-going wave. Obviously, the above equations are of the KP type, and incorporate a dissipative perturbation having the form of a linear loss term. Generally, the KP equation is a 2D extension of the KdV equation—cf. Eq. (29) for $\partial_{\mathcal{Y}} = 0$. The particular form of Eq. (29) is of the KP-I type, i.e., it is characterized by positive dispersion, and is known to govern shallow water waves, in the case where surface tension dominates gravity [28].

Importantly, the KP-I equation is known to display the effect of transverse instability and self-focusing of planar (quasi-1D) localized structures, so-called line solitons (cf. next section). In particular, as was first shown in hydrodynamics and plasma physics [38], line solitons develop undulations and eventually decay into lumps [58]. Additionally, in optics, the asymptotic reduction of the defocusing 2D nonlinear Schrödinger (NLS) equation to KP-I [55,59], and the instability of the line solitons of the latter, was used to better understand the transverse instability of rectilinear dark solitons: indeed, these structures being subject to transverse (alias "snaking") instability, also develop undulations and eventually decay into vortex pairs [55,60] or, in some cases, into 2D vorticity-free structures resembling KP lumps [46]. A recent analysis of the resulting line soliton filament dynamics can be found in Ref. [61].

Below we will present both the unstable 1D solitons and the stable 2D solitons of the KP-I model, namely the lumps. We will focus on the latter, and show that the lump solution of the KP-I equation can be used to construct weakly localized 2D dark solitons of the original model.

III. SOLITON SOLUTIONS

A. Unperturbed soliton solutions

Without loss of generality, let us consider the case of right-going waves and study, at first, the unperturbed version of the KP-I Eq. (29), corresponding to the case where dissipation is absent. We can use the soliton solutions of this reduced model, which we present below, to find approximate soliton solutions of the open dissipative GP Eqs. (3) and (4). Indeed, in terms of the original (dimensionless) variables and coordinates, x, y, and t, one may write down an approximate [up to order $\mathcal{O}(\epsilon)$] solution for the macroscopic wavefunction Ψ of the polariton condensate and the exciton density n_R as follows:

$$\Psi \approx \sqrt{\rho_0 + \epsilon\rho_1^{(R)}}\exp\left(-i\mu t + i\epsilon^{1/2}\Phi_0^{(R)}\right), \tag{30}$$

$$n \approx n_0 - \epsilon\frac{\gamma_C}{\gamma_R}\rho_1^{(R)}, \tag{31}$$

where $\rho_1^{(R)}$ is a soliton of KP-I (29) and $\Phi_0^{(R)}$ is the respective phase, which can be directly found from the first of Eqs. (28).

Let us now present the soliton solutions of the KP-I, Eq. (29), which can be distinguished into two types. The first one which is quasi-1D, and is usually called "line soliton" [28], has the form:

$$\rho_1^{(R)} = -\kappa^2\mathrm{sech}^2 Z, \quad Z = \kappa[\mathcal{X} - \zeta(\mathcal{T})], \tag{32}$$

where κ is a free parameter linking the soliton's amplitude to its velocity, $\zeta(\mathcal{T}) = 4\kappa^2\mathcal{T} + \zeta_0$ is the soliton center (with the constant ζ_0 denoting the initial soliton location), and $d\zeta/d\mathcal{T} = 4\kappa^2$ is the soliton velocity in the $(\xi, \mathcal{T})$ reference frame. The above 1D structure is actually the soliton solution of the KdV equation associated with the KP-I Eq. (29) extended uniformly in the $\mathcal{Y}$ direction. The phase $\Phi_0^{(R)}$ associated to this solution can be obtained from the first of Eqs. (28):

$$\Phi_0^{(R)} = -\frac{\kappa^2}{C}\tanh Z, \tag{33}$$

and it should be mentioned that, in terms of the original (dimensionless) coordinates, x, y, and t, the variable Z reads

$$Z = \epsilon^{1/2}\kappa\left[x - \left(C - \frac{\epsilon\kappa^2}{2C}\right)t - x_0\right]. \tag{34}$$

Clearly, in this case, the solution of Eq. (30) has the form of a sech-shaped density dip, with a tanh-shaped phase jump across the density minimum, and it is thus a dark (gray) soliton. However, the exciton density Eq. (31) follows the form of an antidark soliton, i.e., it has a sech^2 hump shape on top of the background, at the location of the dark polariton soliton, and asymptotes (for $x \to \pm\infty$) to the equilibrium density n_0. Notice that the dynamics of this solution was studied systematically in the context of the 1D analog of the open-dissipative GP model Eqs. (3) and (4) in the recent work of Ref. [27]. Furthermore, in the 2D setting, the transverse instability of 1D dark solitons of a similar form was also studied in the context of exciton-polariton condensates in Ref. [24].

Let us next proceed with the second type of soliton solution of Eq. (29), which is of primary interest herein. This is a genuinely 2D soliton, known as "lump" [28], and is of the form

$$\rho_1^{(R)} = -2\frac{-\left(\xi + \frac{3V}{2C}\mathcal{T}\right)^2 + \frac{3W}{C^2}\mathcal{Y}^2 + \frac{1}{4\beta^2}}{\left[\left(\xi + \frac{3V}{2C}\mathcal{T}\right)^2 + \frac{3W}{C^2}\mathcal{Y}^2 + \frac{1}{4\beta^2}\right]^2}, \tag{35}$$

where β is a free parameter connecting the velocity $(-\frac{3V}{2C})$ and the inverse width through $V = W = \beta^2$ and thus linking the soliton amplitude with its velocity and transverse width. This solution is weakly localized, since it decays algebraically as $(\xi^2 + \mathcal{Y}^2)^{1/2} \to \infty$. Employing, as before, the first of Eqs. (28), we can also obtain the associated phase

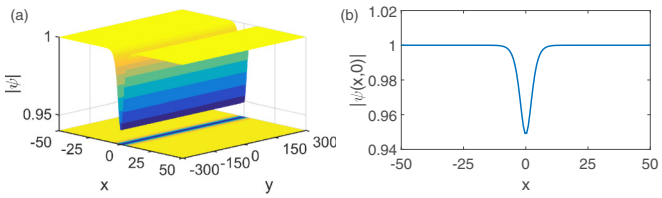

FIG. 1. Three-dimensional plot of the approximate 1D dark stripe soliton [panel (a)] and the respective wave functions' modulus, $|\psi| = |\psi(x, t = 0)|$ [panel (b)]. All quantities with tildes are equal to one, $\gamma_R = g_R = 1$, and $\epsilon = 0.1$; furthermore, $\kappa = 1$.

$\Phi_0^{(R)}(\xi, \mathcal{Y}, \mathcal{T})$:

$$\Phi_0^{(R)} = -\frac{2}{C}\left[\frac{\xi + \frac{3V}{2C}\mathcal{T}}{\left(\xi + \frac{3V}{2C}\mathcal{T}\right)^2 + \frac{3W}{C^2}\mathcal{Y}^2 + \frac{1}{4\beta^2}}\right]. \tag{36}$$

Then, returning to the original (dimensionless) variables and coordinates, x, y, and t, one may express Eqs. (35) and (36) as

$$\rho_1^{(R)} = -2\frac{-\epsilon\left[x - \left(C - \epsilon\frac{V}{8C}\right)t\right]^2 + \epsilon^2\frac{W}{4C^2}y^2 + \frac{3}{\beta^2}}{\left[\epsilon\left[x - \left(C - \epsilon\frac{V}{8C}\right)t\right]^2 + \epsilon^2\frac{W}{4C^2}y^2 + \frac{3}{\beta^2}\right]^2}, \tag{37}$$

$$\Phi_0^{(R)} = \frac{-\frac{2}{C}\epsilon^{1/2}\left[x - \left(C - \epsilon\frac{V}{8C}\right)t\right]}{\epsilon\left[x - \left(C - \epsilon\frac{V}{8C}\right)t\right]^2 + \epsilon^2\frac{W}{4C^2}y^2 + \frac{3}{\beta^2}}. \tag{38}$$

It is clear that upon substituting Eqs. (37) and (38) into Eq. (30), one obtains for the macroscopic wave function Ψ an approximate, vorticity-free, and weakly localized 2D dark soliton, in the form of a dark lump, that decays algebraically as $(x^2 + y^2)^{1/2} \to \infty$. The exciton density n, however, takes the form of an antidark lump on top of the background density n_0, at the location of the dark polariton soliton, and asymptotes (for $x, y \to \pm\infty$) to n_0.

The form of the approximate soliton solutions, namely of the 1D dark stripe soliton and the 2D dark lump soliton, is depicted, respectively, in Figs. 1 and 2. In particular, three-dimensional (3D) plots of the wave functions' moduli are shown, $|\psi| = |\psi(x, t)|$, of the 1D dark soliton stripe (Fig. 1) and the 2D dark lump [Figs. 2(a) and 2(b)], at $t = 0$; notice that the plot depicting the lump's phase profile [Fig. 2(b)] clearly shows that the dark lump is a vorticity-free structure. For clarity, we also show the spatial profiles of $|\psi|$ for the dark lump, at $x = 0$ and $y = 0$ [Figs. 2(c) and 2(d)]. Here, we use the following parameter values: all quantities with tildes are set equal to one, $\gamma_R = g_R = 1$, and $\epsilon = 0.1$. In addition, the characteristic parameters of the dark soliton stripe and the dark lump are, respectively, chosen to be $\kappa = 1$ and $\beta = 1$.

Here, we should also mention the following. Generally, in the context of the defocusing GP equation, there exist stationary (black) dark solitons, characterized by a zero density dip and velocity. Nevertheless, both the line and the lump soliton satisfying the KP-I equation—and, hence, the pertinent approximate solutions of the open dissipative GP model—are genuine traveling waves. This can be seen by the fact that the characteristic parameters κ and β of the dark stripe and the lump soliton, set simultaneously the amplitude and the velocity (as well as the width) of the solutions. Thus, stationary counterparts of these structures do not exist.

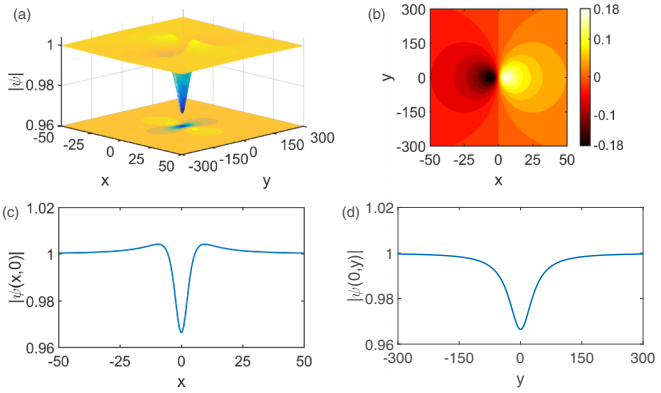

FIG. 2. Top panels: three-dimensional plot of the approximate 2D dark lump soliton solution (left), and a contour plot depicting its phase profile (right). Bottom panels: the wave function's modulus profiles of the dark lump, $\psi(x, y = 0, t = 0)$ (left), and $\psi(x = 0, y, t = 0)$ (right). All quantities with tildes are equal to one, $\gamma_R = g_R = 1$, and $\epsilon = 0.1$; furthermore, $\beta = 1$.

B. Dissipation-induced soliton dynamics

Let us now consider the role of the small dissipative perturbation, in the form of a linear loss term, appearing in the right-hand side of Eq. (29). In both 1D and 2D cases, the evolution of the 1D KdV soliton and the 2D KP-I lump in the presence of the weak linear loss term has been studied by means of various techniques. Let us consider at first the problem of the KdV soliton dynamics in the case $\epsilon \neq 0$, which has been analyzed in the past by using a perturbed inverse scattering transform (IST) theory [62,63] and asymptotic expansion methods [64,65] (see also the review [66]). The main result of the analyses reported in these works is that the soliton has the functional form given in Eq. (32), but the parameter κ setting the amplitude width and velocity of the soliton, becomes time-dependent, reflecting the open-dissipative nature of the dynamics. In particular, in terms of the original time, its evolution is given by the expression

$$\kappa(t) = \kappa(0)\exp(-t/t_\star), \tag{39}$$

where $\kappa(0) \equiv \kappa(t = 0)$, and the soliton decay rate $t_\star$ is given by

$$t_\star = \frac{3}{\alpha\gamma_C}t_0 = \frac{3}{\gamma_C}\frac{P_0^{(\mathrm{th})}}{P_0 - P_0^{(\mathrm{th})}}t_0, \tag{40}$$

where t_0 is the characteristic time scale for the system introduced in Sec. II.

The dissipation-induced dynamics of the lump of the KP-I model has been studied in Ref. [67] by means of the perturbed IST theory. According to this work, in this case too, in the presence of the weak dissipation the parameter the parameter β characterizing the amplitude, width and velocity of the lump becomes a function of time. In terms of the original time, its evolution is given by an expression similar to that in Eq. (40), namely,

$$\beta(t) = \beta(0)\exp(-t/T_\star), \tag{41}$$

where $\beta(0) \equiv \beta(t=0)$, with the lump decay rate $T_\star$ given by

$$T_\star = \frac{1}{\alpha\gamma_C} t_0 = \frac{1}{\gamma_C} \frac{P_0^{(\mathrm{th})}}{P_0 - P_0^{(\mathrm{th})}} t_0. \tag{42}$$

It is observed that, in the weak pumping regime under consideration, both the soliton's and the lump's decay rates depend on the decay rate γ_C of the polariton condensate, as well as the relative deviation α of the uniform pumping P_0 from the threshold value $P_0^{(\mathrm{th})}$. Importantly, it turns out that

$$T_\star = \tfrac{1}{3}\, t_\star, \tag{43}$$

a fact that indicates that the soliton decays faster than the lump. Furthermore, it is relevant to note that the soliton stripe, in addition to the aforementioned decay, is also subject to transverse instabilities, as we will discuss in our numerical results below. Thus, chiefly, the weakly localized 2D dark solitonic structure constitutes the 2D (nonvortical) coherent structure that has the best chance to be observed in realistic physical experiments.

C. Numerical results

Let us now test the validity of our analytical considerations above by contrasting them against direct numerical simulations of the original system of Eqs. (3) and (4). In particular, for this comparison, we will study:

(i) the existence and dissipative dynamics of dark lumps, and

(ii) the spontaneous generation of coherent structures resulting from the snaking instability of dark soliton stripes.

For simplicity, in our simulations, all quantities with tildes have been set equal to unity, namely $\tilde{\alpha} = \tilde{\gamma}_C = \tilde{R} = 1$, as well as $\gamma_R = g_R = 1$. Thus, parameters of the open dissipative GP model, Eqs. (3) and (4), as well as our initial data only depend on the small parameter ϵ. For the initial conditions, we use the analytical form of the dark soliton stripe and dark lump, i.e., Eqs. (30) and (31), with $\rho_1^{(R)}$ and Φ given by Eqs. (32) and (33) for the stripe or by Eqs. (35) and (36) for the lump.

First, we study the existence and dissipative dynamics of dark lumps (for a relevant study for the dark solitons in the 1D setting see Ref. [27]). Since our approach relies on a perturbation method, it is expected that the agreement between analytical and numerical results will be better for relatively smaller values of ϵ; for this reason, we choose $\epsilon = 0.01$. Figure 3 shows snapshots of the dark lump modulus $|\psi(x, y, t)|$ as a function of x (i.e., along the propagation direction), for different time instants, up to $t = 80$. We have obtained similar results (in terms of the quality of the agreement with the theoretical prediction) along the y direction (results not shown here). It is observed that dark lump solitons do exist and they follow dissipative dynamics which is well described by the analytical predictions—compare the numerical [solid (blue) lines] and analytical [dashed (red) lines] profiles of the lump modulus. For this simulation, the relative maximum error in the estimation of the dark lump's minimum at $t = 80$ is less than 3%. We have checked that even for values of ϵ about an order of magnitude larger, the error is approximately 15% (at the same time $t = 80$), while the qualitative characteristics of the lump's evolution are similar to those shown in Fig. 3. In any case, we have found that our analytical approach tends to underestimate the actual dissipation of the dark lump solitons.

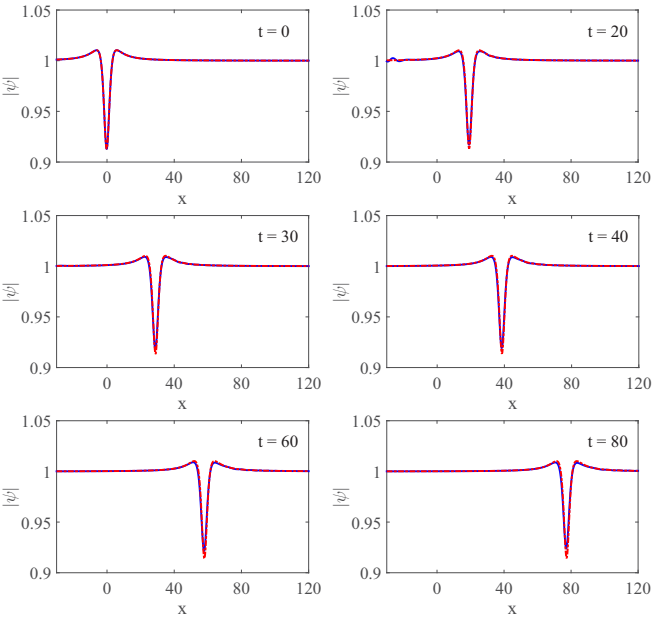

FIG. 3. Evolution of the dark lump soliton. Solid (blue) lines and dashed (red) ones depict, respectively, the numerical and analytical wave function's modulus $|\psi(x, y, t)|$ for $y = 0$. All quantities with tildes are equal to one, $\gamma_R = g_R = 1$, and $\epsilon = 0.01$; furthermore, $\beta(0) = 5$.

Next, having checked the existence and dissipation-induced dynamics of the dark lumps, we now proceed to study the evolution of the dark line (i.e., stripe) solitons. Here, we focus on their spontaneous breakup resulting from the transverse instability. As discussed in the previous section, in the 2D setting, line solitons of KP-I are unstable and decay into lumps [58]. In the context of the defocusing NLS, the snaking instability of dark soliton stripes results in their decay into vortices [59]; this effect was studied in detail also in the context of polariton superfluids [24].

Based on previous results referring to shallow solitons of the 2D NLS [46], we expect that sufficiently deep stripe dark solitons, which are beyond the analytical description of Eqs. (30) and (31) will decay into vortices; on the contrary, sufficiently shallow stripe dark solitons, described by Eqs. (30) and (31), with $\rho_1^{(R)}$ and Φ as given by Eqs. (32) and (33), will develop undulations in 2D and eventually decay into 2D vorticity-free structures resembling the dark lump solitons.

These two scenarios are confirmed by our simulations. Pertinent results are shown in Figs. 4 and 5, corresponding to relatively deep dark soliton stripes, as well as in Figs. 6 and 7, corresponding to shallower dark soliton stripes. In both cases, parameter values were chosen as previously and $\epsilon = 0.1$. To accelerate the onset of the snaking instability, we have transversely perturbed the characteristic parameter of the soliton, κ, thus, using

$$\kappa = \kappa_0 + \kappa_1 \cos(K y), \tag{44}$$

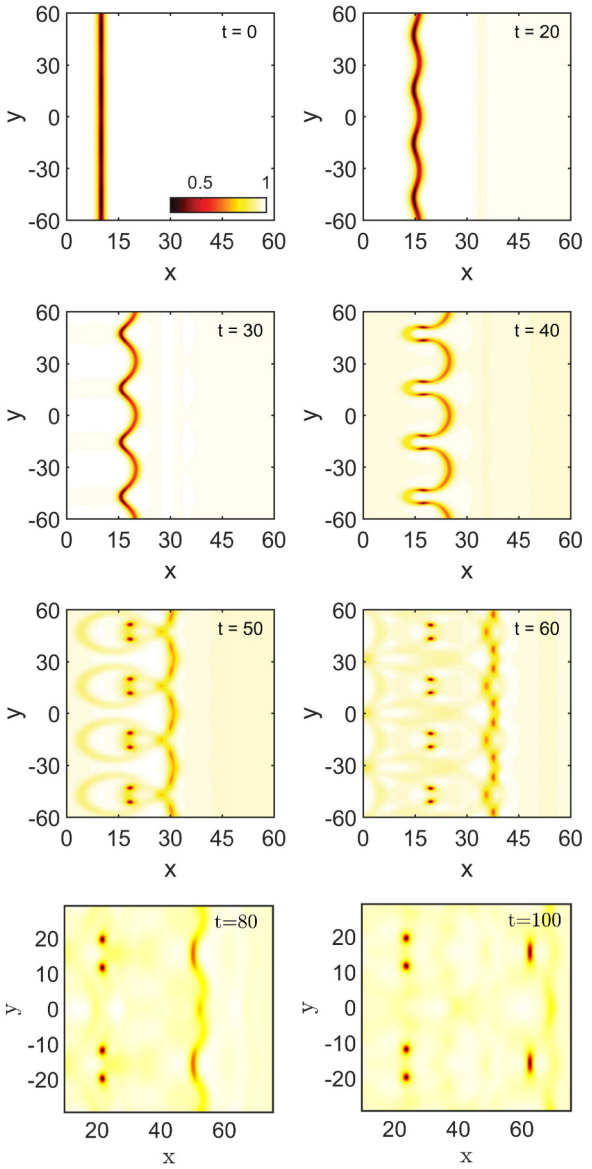

FIG. 4. Evolution of a relatively deep dark soliton stripe undergoing snaking instability. The panels depict the wave function's modulus at the indicated times. Notice that after strong undulation, the stripe decays into vortex pairs, which are formed at approximately $t = 50$. A zoom showing the lowest vortex pair is depicted in Fig. 5. The zooms at later times at $t = 80$ and $t = 100$ (see bottom panels) are intended to demonstrate the redistribution of the original stripe into pairs of vortices and in lumps in this case. All quantities with tildes are equal to one, $\gamma_R = g_R = 1$, and $\epsilon = 0.1$; furthermore, here, $\kappa = 3 + 0.3\cos(0.2y)$.

where the transverse perturbation wave number is set to $K = 0.2$, while $\kappa_0 = 3$ and $\kappa_1 = 0.3$ for Figs. 4 and 5, whereas $\kappa_0 = 4.5$ and $\kappa_1 = 0.4$ for Figs. 6 and 7.

First, Fig. 4 depicts the evolution of a relatively deep dark stripe soliton. It is clearly seen that, after developing strong undulations, the dark soliton stripe is destroyed, and a chain of 2D structures, namely vortex-antivortex pairs, are formed—see, e.g., the snapshot at $t = 50$. In Fig. 5 we depict a zoom of the lowest vortex pair at $t = 60$. This figure clearly shows that indeed, both the phase plot, which is characteristic of a

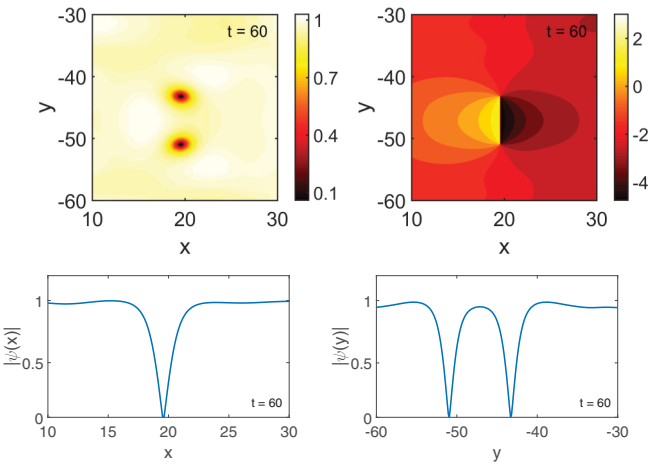

FIG. 5. A zoom depicting the lowest vortex pair shown in Fig. 4 at $t = 60$. The top panels correspond to contour plots of the density (left) and the phase (right); the latter, clearly reveals the phase profile of a vortex-antivortex pair. The bottom panels depict the x (left) and y (right) profiles of wave function's modulus of the vortex pair.

vortex-antivortex pair [Fig. 5(b)], as well as the profiles of the wave function's modulus, justify the formation of vortex pairs in the deep dark soliton stripe case. We note in passing

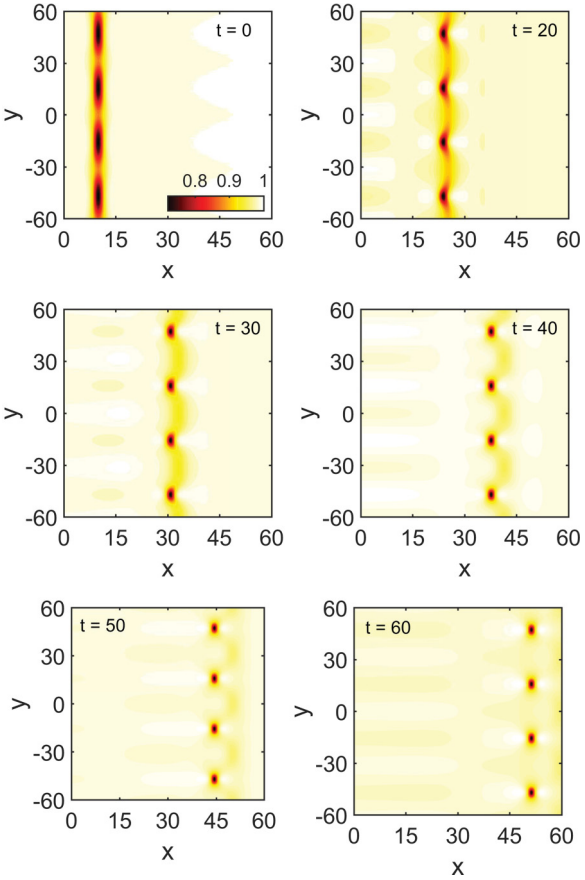

FIG. 6. Same as Fig. 4, but for a relatively shallow dark soliton stripe. In this case, after strong undulation, the stripe decays into dark lumps, which are formed at approximately $t = 50$. A zoom of the lowest lump is shown in Fig. 7. All parameters are the same as in Fig. 4, while here $\kappa = 4.5 + 0.4\cos(0.2y)$.

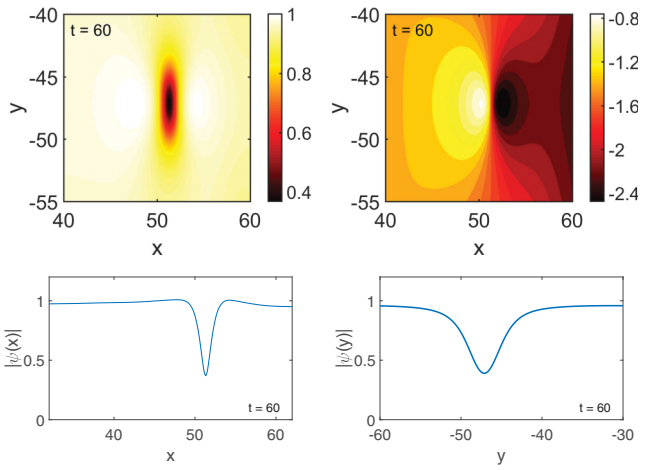

FIG. 7. A zoom depicting the lowest lump shown in Fig. 6 at $t = 60$. Same layout as in Fig. 5. Notice that the panels clearly reveal the profile of a lump as depicted in Fig. 2.

that we have checked that qualitatively similar results pertain also to the case of stationary (black) stripes, which always decay into vortices as well (in accordance with the analysis of Refs. [24,46,55,59,60]).

However, Fig. 6 depicts the evolution of a relatively shallow dark stripe soliton. It is observed that, in this case too, the dark soliton stripe is destroyed after the onset of the snaking instability. Nevertheless, in this case the 2D structures that are formed are dark lump solitons. This becomes evident in Fig. 7 depicting the lowest lump in Fig. 6 for $t = 60$. The figure clearly shows that both the wavefunction's modulus and phase, as well as the x and y profiles, take a form of a genuine dark lump soliton—see Fig. 2 for a comparison.

It is also relevant to note that in Fig. 4, apart from the vortex-antivortex pairs that are formed around $x = 20$ and remain near this position, there are other two-dimensional density dips that continue to travel in the x direction and form a propagating front modulated along the y axis. We have checked that these transient density dips that are formed during the disintegration of the dark soliton do recombine at later times (around $t = 100$, as shown in the bottom-right panel of the figure) to indeed form stable propagating lumps. A detailed study on the critical value of the dark soliton's depth relevant towards eventually generating lump structures falls outside of the scope of the current manuscript and will be studied elsewhere.

Qualitatively similar results have been obtained with other parameter values (results not shown here), a fact that indicates that the dark lump solitons appear generically after the onset of the snaking instability of sufficiently weak dark soliton stripes.

IV. CONCLUSIONS

Employing multiscale expansion methods, we studied the effective hydrodynamic equations resulting from a mean-field model for polariton superfluids. The model consists of an open-dissipative Gross-Pitaevskii equation for the polariton condensate coupled to a rate equation corresponding to the exciton reservoir. We focus on the case of weak uniform pumping and sufficiently small polariton loss and stimulated scattering rates.

In particular, we have derived several model equations that are commonly used in shallow water waves with viscosity—as well as other physical contexts. We have thus first derived, at an intermediate stage, a Boussinesq/Benney-Luke type equation, and then its far-field, a Kadomtsev-Petviashvili-I (KP-I) equation for right- and left-going waves. By means of the KP-I model, we predict the existence of weakly-localized (algebraically decaying) 2D dark-lump solitons. It is found that, in the presence of dissipation, these dark lumps exhibit a lifetime three times larger than that of dark soliton stripes. We argued that on the basis of their robustness (e.g., against transverse undulations) and as a result of their larger lifetime, these lump structures are likely to be observable in 2D exciton-polariton superfluids experiments.

Our analytical predictions were corroborated by direct numerical simulations. We found that, indeed, dark lump solitons do exist and, for sufficiently small values of the formal perturbation parameter, their dissipative dynamics is well described by the analytical estimates. Furthermore, we have shown that dark lump solitons, as well as vortical structures, may emerge spontaneously after the onset of the snaking instability of sufficiently deep dark soliton stripes.

The present results could be particularly interesting to be generalized to the multisoliton solution, also known as "soliton gas" (see Refs. [68,69]). For that, a basic ingredient is the pairwise interaction between solitons [43], and a relevant question is how the dark lump changes the character of this potential. In particular, it may be natural to expect that the algebraic nature of the decay of their tails may lead to an algebraic lump-lump interaction. Recall that similarly algebraic is the nature of vortex-vortex interactions in the NLS, although the latter does not feature a Newtonian particle character [70]. This could be extremely relevant to explore systematically, not only theoretically but also in future experiments.

In addition, it would be interesting to extend our considerations to multicomponent (spinor) polariton superfluid settings—see, e.g., Refs. [7,26,71–73]. In such settings, a quite relevant investigation would concern the existence of spinorial, vorticity-free dark lump solitonic structures.

It should also be interesting to use the methodology devised in this work to study other models that are used in the context of open dissipative systems, such as the Lugiato-Lefever equation [74] describing dissipative dynamics in optical resonators. Note also that in the present setting we have considered homogeneous condensates. However, parabolic as well as periodic potentials are routinely used nowadays in exciton-polariton superfluids. Exploring how such external traps may affect the present phenomenology would also be an interesting direction for future work. Such studies are currently in progress and will be reported in future publications.

ACKNOWLEDGMENTS

A.S.R. acknowledges the financial support from FCT through Grant No. SFRH/BSAB/135213/2017. P.G.K. gratefully acknowledges the support from NSF-PHY-1602994. R.C.G. gratefully acknowledges the support from NSF-PHY-1603058. J.C.-M. thanks the financial support from MAT2016-79866-R project (AEI/FEDER, UE).

[1] H. Deng, H. Haug, and Y. Yamamoto, Rev. Mod. Phys. **82**, 1489 (2010).
[2] I. Carusotto and C. Ciuti, Rev. Mod. Phys. **85**, 299 (2013).
[3] M. Wouters and I. Carusotto, Phys. Rev. Lett. **99**, 140402 (2007).
[4] M. Wouters, I. Carusotto, and C. Ciuti, Phys. Rev. B **77**, 115340 (2008).
[5] S. Pigeon, I. Carusotto, and C. Ciuti, Phys. Rev. B **83**, 144513 (2011).
[6] J. Keeling and N. G. Berloff, Phys. Rev. Lett. **100**, 250401 (2008).
[7] M. O. Borgh, J. Keeling, and N. G. Berloff, Phys. Rev. B **81**, 235302 (2010).
[8] K. G. Lagoudakis, M. Wouters, M. Richard, A. Baas, I. Carusotto, R. Andre, Le Si Dang, and B. Deveaud-Plédran, Nat. Phys. **4**, 706 (2008).
[9] A. Amo, S. Pigeon, D. Sanvitto, V. G. Sala, R. Hivet, I. Carusotto, F. Pisanello, G. Leménager, R. Houdré, E. Giacobino, C. Ciuti, and A. Bramati, Science **332**, 1167 (2011).
[10] G. Roumpos, M. D. Fraser, A. Löffler, S. Höfling, A. Forchel, and Y. Yamamoto, Nat. Phys. **7**, 129 (2011).
[11] L. Dominici, R. Carretero-González, J. Cuevas-Maraver, A. Gianfrate, A. S. Rodrigues, D. J. Frantzeskakis, P. G. Kevrekidis, G. Lerario, D. Ballarini, M. De Giorgi, G. Gigli, and D. Sanvitto, Nat. Comm. **9**, 1467 (2018).
[12] Ye. Larionova, W. Stolz, and C. O. Weiss, Opt. Lett. **33**, 321 (2008).
[13] K. G. Lagoudakis, T. Ostatnický, A. V. Kavokin, Y. G. Rubo, R. André, and B. Deveaud-Plédran, Science **326**, 974 (2009).
[14] G. Grosso, G. Nardin, F. Morier-Genoud, Y. Léger, and B. Deveaud-Plédran, Phys. Rev. Lett. **107**, 245301 (2011).
[15] G. Grosso, G. Nardin, F. Morier-Genoud, Y. Léger, and B. Deveaud-Plédran, Phys. Rev. B **86**, 020509(R) (2012).
[16] L. Dominici, M. Petrov, M. Matuszewski, D. Ballarini, M. De Giorgi, D. Colas, E. Cancellieri, B. Silva Fernández, A. Bramati, G. Gigli, A. Kavokin, F. Laussy, and D. Sanvitto, Nat. Commun. **6**, 8993 (2015).
[17] V. Goblot, H. S. Nguyen, I. Carusotto, E. Galopin, A. Lemaître, I. Sagnes, A. Amo, and J. Bloch, Phys. Rev. Lett. **117**, 217401 (2016).
[18] X. Ma, O. A. Egorov, and S. Schumacher, Phys. Rev. Lett. **118**, 157401 (2017).
[19] A. V. Yulin, O. A. Egorov, F. Lederer, and D. V. Skryabin, Phys. Rev. A **78**, 061801(R) (2008).
[20] A. M. Kamchatnov and S. V. Korneev, J. Exp. Theor. Phys. **115**, 579 (2012).
[21] S. Komineas, S. P. Shipman, and S. Venakides, Phys. Rev. B **91**, 134503 (2015).
[22] J. Cuevas, A. S. Rodrigues, R. Carretero-González, P. G. Kevrekidis, and D. J. Frantzeskakis, Phys. Rev. B **83**, 245140 (2011).
[23] A. S. Rodrigues, P. G. Kevrekidis, R. Carretero-González, J. Cuevas, D. J. Frantzeskakis, and F. Palmero, J. Phys: Cond. Matt. **26**, 155801 (2014).
[24] L. A. Smirnov, D. A. Smirnova, E. A. Ostrovskaya, and Yu. S. Kivshar, Phys. Rev. B **89**, 235310 (2014).
[25] Y. Xue and M. Matuszewski, Phys. Rev. Lett. **112**, 216401 (2014).
[26] F. Pinsker, Annals Phys. **362**, 726 (2015).
[27] R. Carretero-González, J. Cuevas-Maraver, D. J. Frantzeskakis, T. P. Horikis, P. G. Kevrekidis, and A. S. Rodrigues, Phys. Lett. A **381**, 3805 (2017).
[28] M. J. Ablowitz, *Nonlinear Dispersive Waves: Asymptotic Analysis and Solitons* (Cambridge University Press, Cambridge, 2011).
[29] E. Infeld and G. Rowlands, *Nonlinear Waves, Solitons, and Chaos* (Cambridge University Press, Cambridge, 1990).
[30] M. Remoissenet, *Waves Called Solitons* (Springer, Berlin, 1999).
[31] D. J. Benney and J. C. Luke, J. Math. Phys. **43**, 309 (1964).
[32] D. Dutykh and F. Dias, C. R. Mecanique **335**, 559 (2007).
[33] L. Jiang, C.-L. Ting, M. Perlin, and W. W. Schultz, J. Fluid Mech. **329**, 275 (1996).
[34] B. B. Kadomstev and V. I. Petviashvili, Sov. Phys. Dokl. **15**, 539 (1970).
[35] C. J. Knickerbocker and A. C. Newell, J. Fluid. Mech. **153**, 1 (1985).
[36] D. David, D. Levi, and P. Winternitz, Stud. Appl. Math. **76**, 133 (1987).
[37] M. J. Ablowitz and P. A. Clarkson, *Solitons, Nonlinear Evolution Equations, and Inverse Scattering* (Cambridge University Press, Cambridge, 1991).
[38] E. A. Kuznetsov, A. M. Rubenchik, and V. E. Zakharov, Phys. Rep. **142**, 103 (1986).
[39] D. J. Frantzeskakis, K. Hizanidis, B. A. Malomed, and C. Polymilis, Phys. Lett. A **248**, 203 (1998).
[40] C. Polymilis, D. J. Frantzeskakis, A. N. Yannacopoulos, K. Hizanidis, and G. Rowlands, J. Opt. Soc. Am. B **18**, 75 (2001).
[41] F. Baronio, S. Wabnitz, and Y. Kodama, Phys. Rev. Lett. **116**, 173901 (2016).
[42] G. Huang, V. A. Makarov, and M. G. Velarde, Phys. Rev. A **67**, 023604 (2003).
[43] R. Carretero-González, D. J. Frantzeskakis, and P. G. Kevrekidis, Nonlinearity **21**, R139 (2008); D. J. Frantzeskakis, J. Phys. A: Math. Theor. **43**, 213001 (2010).
[44] Yan-Xia Xu and Wen-Shan Duan, Chinese Phys. B **21**, 115202 (2012).
[45] Tian Duo-Xiang, He Guang-Jun, Han Jiu-Ning, and Duan Wen-Shan, Commun. Theor. Phys. **51**, 529 (2009).
[46] V. A. Mironov, A. I. Smirnov, and L. A. Smirnov, Zh. Eksp. Teor. Fiz. **139**, 55 (2011) [J. Exp. Theor. Phys. **112**, 46 (2011)].
[47] G. Verma, U. D. Rapol, and R. Nath, Phys. Rev. A **95**, 043618 (2017).
[48] L. A. Smirnov and V. A. Mironov, Phys. Rev. A **85**, 053620 (2012).
[49] L. A. Smirnov and A. I. Smirnov, Phys. Rev. A **92**, 013636 (2015).
[50] A. J. Groszek, T. P. Simula, D. M. Paganin, and K. Helmerson, Phys. Rev. A **93**, 043614 (2016).
[51] M. Sich, D. V. Skryavin, and D. N. Krizhanovskii, C. R. Physique **17**, 908 (2016).
[52] D. D. Solnyshkov, H. Terças, K. Dini, and G. Malpuech, Phys. Rev. A **89**, 033626 (2014).
[53] J. Kasprzak, M. Richard, S. Kundermann, A. Baas, P. Jeambrun, J. M. J. Keeling, F. M. Marchetti, M. H. Szymańska, R. André, J. L. Staehli, V. Savona, P. B. Littlewood, B. Deveaud, and L. S. Dang, Nature (London) **443**, 409 (2006); R. Balili, V. Hartwell, D. Snoke, L. Pfeiffer, and K. West, Science **316**, 1007 (2007); G. Roumpos, M. Lohse, W. H. Nitsche, J. Keeling,

M. H. Szymańska, P. B. Littlewood, A. Löffler, S. Höfling, L. Worschech, A. Forchel, and Y. Yamamoto, Proc. Nat. Acad. Sci. USA **109**, 6467 (2012).
[54] N. Bobrovska, M. Matuszewski, K. S. Daskalakis, S. A. Maier, and S. Kéna-Cohen, ACS Photonics **5**, 111 (2018).
[55] D. E. Pelinovsky, Yu. A. Stepanyants, and Yu. S. Kivshar, Phys. Rev. E **51**, 5016 (1995).
[56] T. P. Horikis and D. J. Frantzeskakis, J. Phys. A: Math. Theor. **49**, 205202 (2016).
[57] T. P. Horikis and D. J. Frantzeskakis, Phys. Rev. Lett. **118**, 243903 (2017).
[58] E. Infeld, A. Senatorski, and A. A. Skorupski, Phys. Rev. Lett. **72**, 1345 (1994).
[59] E. A. Kuznetsov and S. K. Turitsyn, Zh. Eksp. Teor. Fiz. **94**, 119 (1988) [Sov. Phys. JETP **67**, 1583 (1988)].
[60] Yu. S. Kivshar and D. E. Pelinovsky, Phys. Rep. **331**, 117 (2000).
[61] P. G. Kevrekidis, W. Wang, R. Carretero-González, and D. J. Frantzeskakis, Phys. Rev. Lett. **118**, 244101 (2017).
[62] V. I. Karpman and E. M. Maslov, Zh. Eksp. Teor. Fiz. **73**, 537 (1977) [Sov. Phys. JETP **46**, 281 (1977)]; V. I. Karpman, Phys. Scr. **20**, 462 (1979).
[63] D. J. Kaup and A. C. Newell, Proc. R. Soc. London A **361**, 413 (1978).
[64] K. Ko and H. H. Kuehl, Phys. Rev. Lett. **40**, 233 (1978).
[65] Y. Kodama and M. J. Ablowitz, Stud. Appl. Math. **64**, 225 (1981).
[66] Yu. S. Kivshar and B. A. Malomed, Rev. Mod. Phys. **61**, 763 (1989).
[67] E. S. Benilov and S. P. Burtsev, J. Phys. A: Math. Gen. **19**, L177 (1986).
[68] H. Terças, D. D. Solnyshkov, and G. Malpuech, Phys. Rev. Lett. **110**, 035303 (2013).
[69] H. Terças, D. D. Solnyshkov, and G. Malpuech, Phys. Rev. Lett. **113**, 036403 (2014).
[70] L. M. Pismen, *Vortices in Nonlinear Fields* (Clarendon, Oxford, 1999).
[71] I. A. Shelykh, Yu. G. Rubo, G. Malpuech, D. D. Solnyshkov, and A. Kavokin, Phys. Rev. Lett. **97**, 066402 (2006).
[72] A. Werner, O. A. Egorov, and F. Lederer, Phys. Rev. B **85**, 115315 (2012).
[73] G. Li, T. C. H. Liew, O. A. Egorov, and E. A. Ostrovskaya, Phys. Rev. B **92**, 064304 (2015).
[74] L. A. Lugiato and R. Lefever, Phys. Rev. Lett. **58**, 2209 (1987).